Cell, Vol. 120, 99–110, January 14, 2005, Copyright ©2005 by Elsevier Inc. DOI 10.1016/j.cell.2004.11.032

Coordinated Remodeling of Cellular Metabolism during Iron Deficiency through Targeted mRNA Degradation

Sergi Puig,[1,2] Eric Askeland,[1] and Dennis J. Thiele[1,*]
[1]Department of Pharmacology and Cancer Biology
Sarah W. Stedman Nutrition and Metabolism Center
Duke University Medical Center
Research Drive-LSRC-C351
Durham, North Carolina 27710

Summary

Iron (Fe) is an essential micronutrient for virtually all organisms and serves as a cofactor for a wide variety of vital cellular processes. Although Fe deficiency is the primary nutritional disorder in the world, cellular responses to Fe deprivation are poorly understood. We have discovered a posttranscriptional regulatory process controlled by Fe deficiency, which coordinately drives widespread metabolic reprogramming. We demonstrate that, in response to Fe deficiency, the *Saccharomyces cerevisiae* Cth2 protein specifically downregulates mRNAs encoding proteins that participate in many Fe-dependent processes. mRNA turnover requires the binding of Cth2, an RNA binding protein conserved in plants and mammals, to specific AU-rich elements in the 3′ untranslated region of mRNAs targeted for degradation. These studies elucidate coordinated global metabolic reprogramming in response to Fe deficiency and identify a mechanism for achieving this by targeting specific mRNA molecules for degradation, thereby facilitating the utilization of limited cellular Fe levels.

Introduction

Iron (Fe) is an essential nutrient for virtually all organisms. Fe serves as a cofactor for a wide variety of cellular processes, including oxygen transport, cellular respiration, the tricarboxylic acid (TCA) cycle, lipid metabolism, synthesis of metabolic intermediates, gene regulation, and DNA replication and repair. Despite its abundance in the earth's crust, Fe bioavailability is highly restricted due to its extreme insolubility at physiological pH. Indeed, Fe deficiency is the primary nutritional disorder in the world, estimated to affect over two billion people and resulting in iron deficiency anemia (Baynes and Bothwell, 1990). Alterations in iron homeostasis underlie many human diseases, including Friedreich's ataxia, hereditary hemochromatosis, aceruloplasminemia, Parkinson's disease, aging, microbial pathogenesis, and cancer (Hentze et al., 2004; Nittis and Gitlin, 2002; Roy and Andrews, 2001).

Elegant genetic, biochemical, and physiological studies have elucidated many of the components that function in Fe uptake, efflux, and distribution and their mechanisms of action in both prokaryotic and eukaryotic cells (Escolar et al., 1999; Hentze et al., 2004; Van Ho et al., 2002). Studies with the baker's yeast *Saccharomyces cerevisiae* have demonstrated that, in response to Fe deprivation, cells utilize the Fe-responsive transcription factors Aft1 and Aft2 to induce expression of the so-called iron regulon (Rutherford et al., 2003; Shakoury-Elizeh et al., 2004), which includes proteins involved in Fe reduction at the plasma membrane, uptake, mobilization from intracellular stores, and utilization from heme, among others (Van Ho et al., 2002). Less attention has been dedicated to the characterization of metabolic pathways that are specifically downregulated by Fe depletion. Recent studies have shown that mRNA levels of genes involved in biotin synthesis, glutamate metabolism and heme assembly are downregulated under low Fe conditions (Lesuisse et al., 2003; Shakoury-Elizeh et al., 2004). However, the mechanisms controlling the Fe deprivation-dependent downregulation of these genes, and other global metabolic pathways altered as a consequence of Fe deficiency, have not been elucidated.

In mammals, one response to iron scarcity is posttranscriptionally controlled by the iron-regulatory proteins IRP1 and IRP2. In response to Fe deprivation, IRP1 binds to specific mRNA stem-loop structures known as iron-responsive elements (IREs). IRP1 binding to IREs in the 5′ untranslated region inhibits translation of erythroid aminolevulinic acid synthase, mitochondrial aconitase, the ferroportin Fe efflux pump, and subunits of the Fe storage protein ferritin. IRP1 binding to IREs in the 3′ untranslated region (3′UTR) of the transferrin receptor 1 isoform stabilizes the mRNA, thereby increasing protein levels and enhancing Fe uptake via Fe loaded transferrin (Hentze et al., 2004; Theil, 2000). A posttranscriptional downregulation of Fe-dependent pathways, which depends on small antisense RNAs, has recently been described in bacteria (Masse and Gottesman, 2002; Wilderman et al., 2004).

While several dozen metabolic enzymes require Fe for catalysis in eukaryotic cells, little is known about global reprogramming and regulatory mechanisms governing this process in response to Fe deficiency. We have discovered a mechanism that mediates global posttranscriptional control of multiple components of Fe-dependent pathways to respond in a concerted fashion to Fe deficiency. The Fe-regulated protein Cth2 coordinates this process by binding to and targeting specific mRNA molecules for degradation under Fe deficiency, thereby facilitating the utilization of limited available Fe for normal growth.

Results

Genome-Wide Response of *Saccharomyces cerevisiae* to Iron Deprivation

Although Fe plays a crucial role in a wide array of cellular processes, little is known about how Fe deprivation affects metabolic pathways on a global scale in eukaryotic

*Correspondence: dennis.thiele@duke.edu
[2]Present address: Departament de Bioquimica i Biologia Molecular,

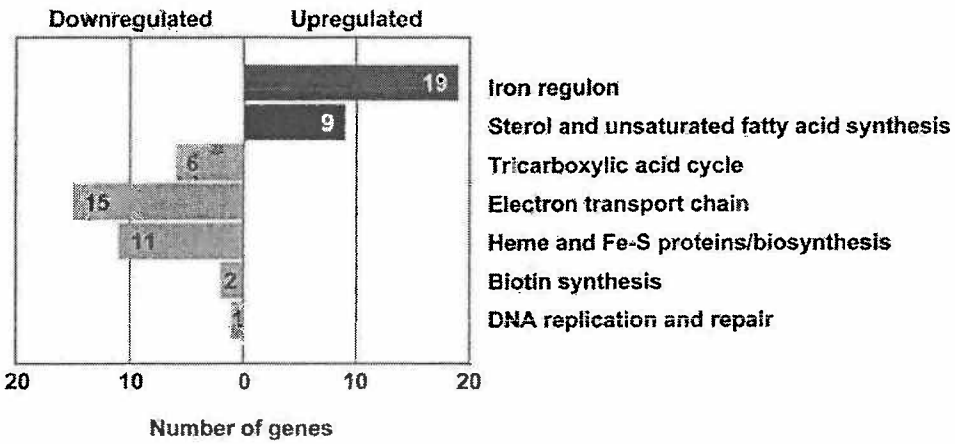

Figure 1. Response of Fe-Dependent Processes to Fe Depletion in Yeast

B4741 wild-type cells were grown in SC containing 300 μM Fe or 100 μM BPS, and RNA was analyzed with DNA microarrays as detailed in Experimental Procedures. Only components of multiple Fe-dependent pathways with a fold change greater than two have been represented. A list of the genes grouped in each functional family is shown in Supplemental Tables S2 and S3.

deprivation, we compared the mRNA expression profile of wild-type cells grown under Fe-replete conditions to cells grown under Fe scarcity achieved by addition of the Fe(II) chelator bathophenantholine disulfonic acid (BPS). We observed that, in addition to changes in other processes (data not shown), key components of multiple Fe-dependent metabolic pathways are significantly altered by Fe availability (Figure 1 and see Supplemental Tables S2 and S3 at http://www.cell.com/cgi/content/full/120/1/99/DC1/). In addition to the induction of the Aft1/2-dependent Fe regulon previously described (Blaiseau et al., 2001; Rutherford et al., 2003; Shakoury-Elizeh et al., 2004; Yamaguchi-Iwai et al., 1996), genes involved in sterol biosynthesis (*ERG* genes) and the fatty acid desaturase *OLE1* are induced under Fe deprivation. In addition, key components of multiple Fe-dependent pathways and proteins including (1) the TCA cycle; (2) the mitochondrial electron transport chain; (3) Fe-S cluster, di-Fe-tyrosyl, and heme-containing proteins; and, (4) as recently described (Lesuisse et al., 2003; Shakoury-Elizeh et al., 2004), *HEM15* encoding ferrochelatase, the last step in heme biosynthesis, and two enzymes involved in biotin synthesis are coordinately downregulated by Fe depletion (Figure 1 and Supplemental Table S3). Taken together, these results demonstrate that mRNA levels of multiple components of Fe-dependent metabolic pathways in *S. cerevisiae* are coordinately regulated in response to Fe deprivation.

The Aft1-Aft2 Target *CTH2* Is Important for Growth under Fe Limitation

Previous DNA microarray experiments strongly suggest that the *CTH2* gene, which encodes a protein related to the mammalian tandem zinc finger (TZF) protein tristetraprolin or TTP (Figure 2A), is transcriptionally induced under Fe limitation (Foury and Talibi, 2001; Rutherford et al., 2003; Shakoury-Elizeh et al., 2004). As shown in Figures 2B and 2C, the steady-state levels of *CTH2* mRNA and a functional FLAG epitope-tagged Cth2 protein under Fe-adequate conditions are very low but dramatically increase in response to Fe deprivation. Furthermore, *CTH2* expression under low Fe conditions is significantly decreased in an *aft1* strain and is undetectable under either condition in the *aft1aft2* double mutant. Mutagenesis of two putative Aft1-Aft2 binding sites (Yamaguchi-Iwai et al., 1996) from the *CTH2* upstream sequence indicates that both sites cooperate in the activation of *CTH2* by Fe starvation, although these experiments do not exclude the participation of other *cis*-regulatory sequences in *CTH2* regulation by Fe (see Supplemental Figure S2 on the *Cell* web site).

Given that *CTH2* mRNA levels are tightly regulated by Fe availability and the Aft1-Aft2 Fe-responsive transcription factors, we assayed growth of *cth2* deletion mutant cells under Fe deprivation conditions. *cth2* cells exhibited a growth defect compared to wild-type cells in the presence of the intracellular Fe-specific chelator ferrozine (Figure 3A). The *cth2* growth defect on ferrozine was reversed by addition of Fe (Figure 3A), demonstrating that the growth defect of *cth2* cells occurs in response to Fe deprivation rather than to ferrozine administration. The yeast genome harbors a gene encoding a protein similar to Cth2, Cth1 (Thompson et al., 1996), whose transcription is independent of Fe levels (Figure 2B). Although *cth1* cells did not display a growth defect under Fe deprivation conditions, cells lacking both *CTH1* and *CTH2* exhibited a more severe growth defect than those lacking only *CTH2* (Figure 3A). Similarly, the *cth1cth2* growth defect in the presence of ferrozine was partially suppressed by *CTH1* and completely recovered by coexpression of both *CTH1* and *CTH2* (Figure 3B). These results demonstrate that *CTH2* is important for growth under Fe deprivation induced by the membrane permeable Fe chelator ferrozine and suggest that Cth1 function in yeast cells may partially overlap with Cth2.

CTH2 Coordinates the Downregulation of Multiple Fe-Dependent Pathways under Fe Deprivation

A prominent feature of Cth2 is the presence of a $Cx_8Cx_5Cx_3H$ tandem zinc finger (TZF) domain near the carboxyl terminus of the protein (Figure 2A and Supplemental Figure S1). This TZF motif is present in a family of

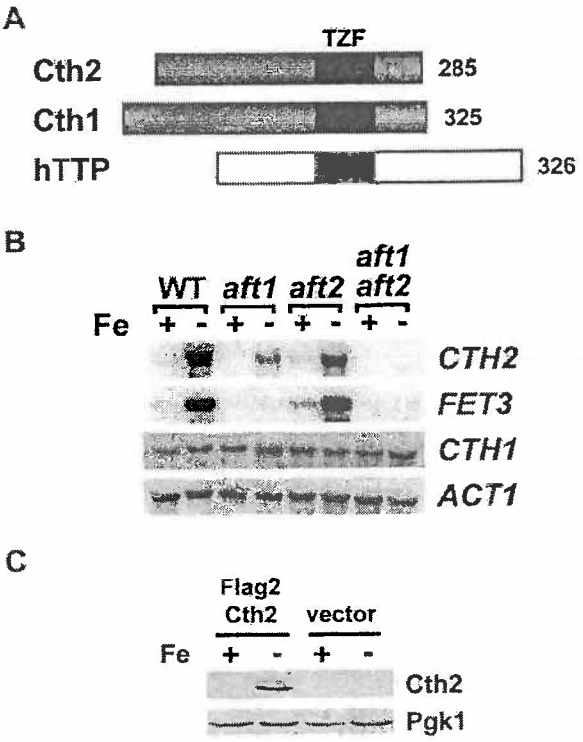

Figure 2. Expression of *CTH2* upon Fe Depletion Is Dependent on Both Aft1 and Aft2 Transcription Factors

(A) Model for the primary structure of *S. cerevisiae* Cth2 and Cth1 and human tristetraprolin (hTTP) protein. TZF, tandem zinc finger.

(B) CM3260 wild-type, *aft1*, *aft2*, and *aft1aft2* cells were grown in SC containing 100 μM Fe (Fe +) or 100 μM BPS (Fe −) and RNA extracted and analyzed by RNA blotting. The Aft1 target *FET3* was used as a control for Fe-regulated expression.

(C) *cth1cth2* cells transformed with pRS416-FLAG2-CTH2 or pRS416 (vector) were grown in SC-Ura containing 300 μM Fe (Fe +) or 100 μM BPS (Fe −) and protein extracted and analyzed by immunoblotting. Phosphoglycerate kinase (Pgk1) was used as a loading control.

RNA binding proteins typified by the mammalian protein tristetraprolin (TTP). TTP mediates the targeted destabilization of tumor necrosis factor α (TNFα), cyclooxygenase-2, interleukin-3, and granulocyte/macrophage colony-stimulating factor (GM-CSF) mRNAs (Blackshear, 2002; Carballo et al., 1998; Sawaoka et al., 2003; Stoecklin et al., 2001). An alignment of yeast Cth1 and Cth2 with human TTP shows that, while Cth1 and Cth2 proteins share 46% identity, hTTP homology to Cth1 and Cth2 is restricted to the TZF domains (Supplemental Figure S1). Despite little homology in the rest of the protein, we hypothesized that Cth2 could be involved in posttranscriptional regulation of specific mRNAs under Fe deprivation. To test this hypothesis, we ascertained the effect of Cth2 on multiple mRNAs we observed in our microarray to be downregulated by Fe deficiency. As shown in Figure 3C, genes encoding proteins involved in the TCA cycle (*SDH4*), heme synthesis (*HEM15*), Fe-S cluster assembly (*ISA1*), vacuolar Fe accumulation (*CCC1*), and Fe-S proteins (*LIP5*) are dramatically downregulated under Fe starvation in a wild-type cleotide reductase, are only modestly decreased by Fe deprivation (Figure 3C). Interestingly, this coordinated mRNA downregulation does not occur in the absence of *CTH2* (Figure 3C, wt versus *cth2* mutant). While mRNA levels in *cth1* cells did not change significantly with respect to wild-type cells, the *cth1cth2* mutant displayed reduced mRNA downregulation, suggesting that Cth1 directly or indirectly influences in this process. These results demonstrate that Cth2 functions in the downregulation of specific mRNAs under conditions of Fe deprivation.

We used DNA microarrays to ascertain which mRNAs exhibit *CTH2*-dependent changes on a genome-wide scale by comparing the gene expression profiles under Fe deficiency of *cth1cth2* cells expressing a plasmid-borne *CTH2* gene or transformed with vector alone. Messenger RNAs corresponding to 84 genes were significantly upregulated in the absence of *CTH2* (Table 1). Interestingly, 54% (45 of 84) of the upregulated genes are involved in obvious Fe-dependent processes, 14% (12 of 84) have other functions, and 32% (27 of 87) are genes of unknown function. Among the 45 Fe-related genes whose expression is increased in *cth2* mutants under low Fe conditions compared to wild-type cells, we find (1) three members of the Fe regulon (*FIT1*, *FIT2*, and *HMX1*); (2) genes encoding key enzymes involved in heme biosynthesis (*HEM15*); (3) two genes encoding proteins involved in Fe-S cluster assembly (*ISA1* and *NFU1*); (4) eight genes encoding enzymes that participate in the TCA cycle including aconitase (*ACO1*), succinate dehydrogenase subunits *SDH2* and *SDH4*, α-ketoglutarate dehydrogenase (*KGD1*), and dihydrolypoyl transsuccinylase (*KGD2*); (5) 15 genes encoding proteins that participate in the electron transfer chain that include four subunits of the cytocrome c oxidase (*COX4*, *COX6*, *COX8*, *COX9*) and six subunits of the ubiquinol cytochrome c reductase complex (*COR1-5* and *RIP1*); (6) eight members of the sterol and unsaturated fatty acid synthesis and metabolism pathways (*ERG* genes and *OLE1*); (7) ribonucleotide-diphosphate reductase subunits (*RNR4*); and (8) genes encoding additional Fe-S cluster-containing proteins (*LIP5*, encoding lipoic acid synthase; *LEU1*, required for leucine biosynthesis; and *RLI1*, related to RNase L inhibitor). Taken together, these results demonstrate that Cth2 functions in the coordinated downregulation of multiple Fe-dependent metabolic pathways, and potentially other as yet uncharacterized pathways, in yeast under conditions of Fe deficiency.

A Conserved RNA Binding Motif Is Required for Cth2-Mediated mRNA Downregulation

Studies with TTP in mammalian systems have demonstrated that the integrity of the zinc finger domains is required for binding and destabilization of specific mRNAs (Blackshear, 2002; Lai et al., 1999, 2003). We tested the role of the CCCH zinc fingers in Cth2-dependent mRNA downregulation by mutagenizing conserved cysteine residues, located in both zinc finger motifs, to arginine. First, cells expressing *CTH2-C190R* or *CTH2-C213R* mutant alleles displayed a growth defect in the

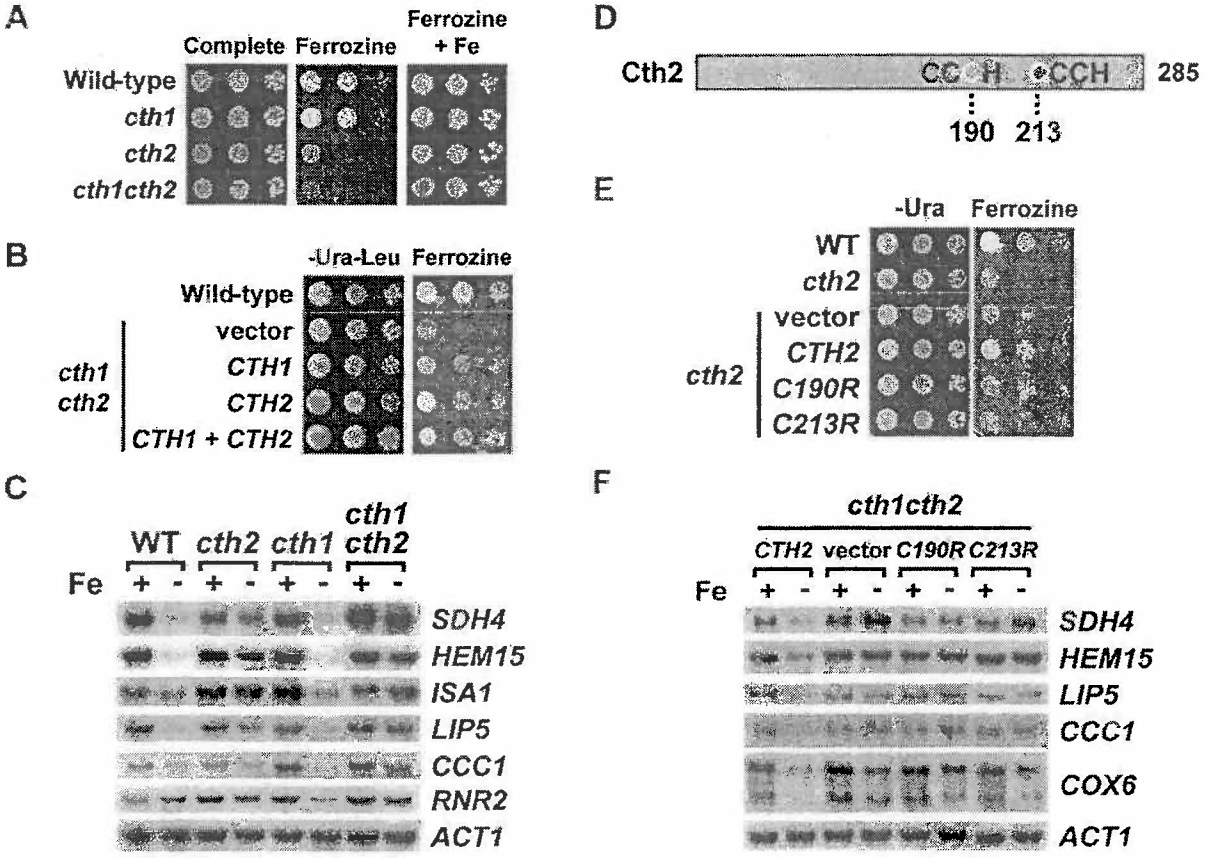

Figure 3. *CTH2* Is Required for Fe-Limited Growth and Fe Deficiency-Dependent mRNA Downregulation

(A) BY4741 wild-type, *cth1*, *cth2*, and *cth1cth2* cells were assayed for growth on SC (Complete) and SC containing 750 μM ferrozine without or with 300 μM Fe (+ Fe).

(B) *cth1cth2* cells cotransformed with pRS416 plus pRS415 (vector), pRS416-CTH1 plus pRS415 (*CTH1*), pRS416 plus pRS415-CTH2 (*CTH2*), and pRS416-CTH1 plus pRS415-CTH2 (*CTH1* + *CTH2*) were assayed on SC-Ura-Leu (−Ura − Leu) and SC containing 750 μM ferrozine.

(C) *CTH2* is essential for Fe deficiency-dependent mRNA downregulation. Wild-type *cth2*, *cth1*, and *cth1cth2* cells were grown in SC media containing 300 μM Fe (Fe +) or 100 μM BPS (Fe −) and RNA extracted and analyzed by RNA blotting.

(D) Schematic representation of the CCCH TZF domain in Cth2 protein. Cysteine residues 190 and 213 (white characters) were mutagenized to arginine.

(E) The Cth2 TZF domains are essential for growth in the presence of ferrozine. BY4741 wild-type and *cth2* cells transformed with vector alone or expressing *CTH2*, *CTH2-C190R*, and *CTH2-C213R* alleles were assayed for growth on ferrozine plates.

(F) The Cth2 CCCH TZF motifs are essential for mRNA downregulation. *cth1cth2* cells containing vector or expressing *CTH2*, *CTH2-C190R*, and *CTH2-C213R* alleles were analyzed by RNA blotting as described for (C).

LIP5, *COX6*, and other mRNAs (data not shown) was abrogated in both Cth2 mutants (Figure 3F). Similar results were obtained when cysteine residues 190 and 213 were mutagenized to alanine (data not shown). Control experiments showed that the cysteine mutant proteins are properly expressed (data not shown). Taken together, these results demonstrate that the integrity of both CCCH zinc finger motifs is essential for Cth2 function in coordinated mRNA downregulation in response to Fe deprivation.

Downregulation of Specific mRNAs by Fe Deprivation Requires AU-Rich Elements

Human TTP binds to AU-rich elements (AREs) within the 3′UTR of target mRNAs and induces RNA degradation (Blackshear et al., 2003; Lai et al., 1999). Interestingly, in silico analysis and visual inspection reveals that approximately 80% of the mRNAs upregulated in *cth2* cells under low Fe conditions contain one or more putative AREs, defined as 5′-UAUUUAUU-3′ and 5′-UUAUU UAU-3′ octamer sequences, located within 500 nucleotides after the translation termination codon (Table 1). To test whether Cth2-dependent mRNA downregulation during Fe deficiency occurs via AREs located within the 3′UTR, we used the mRNA encoding the membrane-anchored heme-containing subunit of the succinate dehydrogenase complex in mitochondria, *SDH4*, which is downregulated under Fe deprivation in a manner completely dependent on Cth2 (Figures 3C and 3F). The *SDH4* 3′UTR contains three 5′-UUAUUUAUU-3′ sequences beginning at 125, 135, and 158 nucleotides after the translation termination codon (Table 1 and Figure 4A). The adenine nucleotides 127, 134, 141, and 160 were mutated to cytosine in a plasmid-borne copy of the *SDH4* gene (Figures 4A and 4B, *SDH4*-AREmt2) and mRNA levels assessed under high and low Fe conditions

Table 1. Genes Upregulated in *cth2* versus Wild-Type Cells under Fe-Limiting Conditions

ORF	Gene	Function	Fold ± SD	Putative AREs
Iron regulon				
YDR534C	FIT1	Cell wall mannoprotein involved in siderophore-Fe uptake	2.0 ± 0.2	263
YOR382W	FIT2	Cell wall mannoprotein involved in siderophore-Fe uptake	1.6 ± 0.1	*255*
YLR205C	HMX1	Heme binding peroxidase involved in reutilization of heme Fe	2.0 ± 0.4	
Heme biosynthesis				
YDR044W	HEM13	Coproporphyrinogen III oxidase, oxygen-requiring enzyme	1.5 ± 0.3[a]	*68, 89*
YOR176W	HEM15	Ferrochelatase, catalyzes insertion of Fe(II) into protoporphyrin IX	2.2 ± 0.2	43, 99
Fe-S cluster biogenesis				
YKL040C	NFU1	NifU-like protein	2.0 ± 0.2	191, 203
YLL027W	ISA1	Member of Fe-S cluster biosynthesis machinery	1.9 ± 0.1	46, 62
TCA cycle				
YNR001C	CIT1	Citrate synthase	2.0 ± 0.2	
YPR001W	CIT3	Mitochondrial isoform of citrate synthase	1.7 ± 0.4	
YLR304C	ACO1	Mitochondrial aconitase, Fe-S cluster protein	2.6 ± 0.3	32, 150, 177
YIL125W	KGD1	Alpha-ketoglutarate dehydrogenase	1.6 ± 0.2	*193, 230*
YDR148C	KGD2	Dihydrolipoyl transsuccinylase	1.8 ± 0.2	242
YLL041C	SDH2	Succinate dehydrogenase (ubiquinone) Fe-S cluster subunit	2.8 ± 0.6	162, *309, 328*
YDR178W	SDH4	Succinate dehydrogenase membrane anchor heme-binding subunit	3.2 ± 0.7	125, 135, 158
YPL262W	FUM1	Mitochondrial and cytoplasmic fumarase, Fe-S cluster protein	1.6 ± 0.2	
Mitochondrial respiration/electron transport chain				
Cytochrome c oxidase				
YGL187C	COX4	Subunit IV of cytochrome c oxidase	1.9 ± 0.4	53
YHR051W	COX6	Subunit VI of cytochrome c oxidase	2.2 ± 0.2	88
YLR395C	COX8	Subunit VIII of cytochrome c oxidase	1.9 ± 0.2	104
YDL067C	COX9	Subunit VIIa of cytochrome c oxidase	1.8 ± 0.2	44
Ubiquinol cytochrome c reductase				
YBL045C	QCR1/COR1	Core subunit I of ubiquinol cytochrome c reductase complex	2.0 ± 0.2	140
YPR191W	QCR2/COR2	Core subunit II of ubiquinol cytochrome c reductase complex	1.6 ± 0.2	155
YFR033C	QCR6/COR3	Subunit VI of ubiquinol cytochrome c reductase complex	1.7 ± 0.3	31
YDR529C	QCR7/COR4	Subunit VII of ubiquinol cytochrome c reductase complex	1.9 ± 0.2	150, *239*
YJL166W	QCR8/COR5	Subunit VIII of ubiquinol cytochrome c reductase complex	1.8 ± 0.3	97, 114
YEL024W	RIP1	Rieske Fe-S protein of ubiquinol cytochrome c reductase complex	2.0 ± 0.1	*293, 355*
YOR356W		Putative mitochondrial dehydrogenase flavoprotein	2.1 ± 0.2	13, 37, 81
YGR255C	COQ6	Flavin-dependent monooxygenase, ubiquinone biosynthesis	1.7 ± 0.3	42
YKR066C	CCP1	Cytochrome c peroxidase	2.8 ± 0.5	18, *41, 50, 59*
YMR145C	NDE1	NADH dehydrogenase	1.6 ± 0.2	
YBL030C	PET9/AAC2	Mitochondrial ADP/ATP carrier	1.6 ± 0.2	
Sterol and fatty acid synthesis and metabolism				
YHR072W	ERG7	Lanosterol synthase	2.0 ± 0.3	*4, 60*
YHR007C	ERG11	Lanosterol C-14 demethylase	1.6 ± 0.1	*174, 203, 273*
YMR208W	ERG12	Mevalonate kinase	1.6 ± 0.1	19
YGR060W	ERG25	C-4 methyl sterol oxidase	1.7 ± 0.4	
YER044C	ERG28	ER membrane protein, may facilitate Erg26 and Erg27 interactions	1.6 ± 0.3	*52*
YGL055W	OLE1	Fatty acid desaturase	1.6 ± 0.3	151, *187*
YMR272C	FAH1/SCS7	Hydroxylation of C-26 fatty acid in ceramide	1.7 ± 0.2	*89, 105*
YPL170W	DAP1	Damage response protein involved in sterol synthesis	1.6 ± 0.1	18, *148*
DNA replication and repair				
YJL026W	RNR2	Ribonucleotide-diphosphate reductase, di-Fe-tyrosyl cofactor	1.4 ± 0.2[a]	68
YGR180C	RNR4	Ribonucleotide-diphosphate reductase, Y4 subunit	1.6 ± 0.4	*39, 125*
Other Fe-, Cu-, and oxygen-related function				
YLR220W	CCC1	Transporter that mediates vacuolar Fe storage	1.4 ± 0.1[a]	*24, 144*
YOR196C	LIP5	Lipoic acid synthase, Fe-S cluster protein	2.0 ± 0.3	70, 92
YGL009C	LEU1	Isopropylmalate isomerase, Fe-S cluster protein	1.7 ± 0.3	85, 123
YDR091C	RLI1	RNase L inhibitor, Fe-S cluster protein	1.6 ± 0.2	*280, 291*
YKL109W	HAP4	Subunit of Hap transcriptional activator	1.7 ± 0.3	*275*, 303
YHR055C	CUP1-2	Copper-binding metallothionein	1.6 ± 0.4	
YAR020C	PAU7	Member of PAU family	1.7 ± 0.2	
YOR394W		Member of PAU family	1.6 ± 0.2	
Other functions				
YCR005C	CIT2	Nonmitochondrial citrate synthase	1.6 ± 0.3	
YDR007W	TRP1	Phosphoribosylanthranilate isomerase	1.8 ± 0.2	*16*
YDR423C	CAD1	Leucine zipper transcriptional activator	1.6 ± 0.3	
YER003C	PMI40	Phosphomannose isomerase	1.6 ± 0.2	54
YHR002W	LEU5	Mitochondrial carrier protein	1.6 ± 0.3	

DOCKET ALARM

Explore Litigation Insights

Docket Alarm provides insights to develop a more informed litigation strategy and the peace of mind of knowing you're on top of things.

Real-Time Litigation Alerts

Keep your litigation team up-to-date with **real-time alerts** and advanced team management tools built for the enterprise, all while greatly reducing PACER spend.

Our comprehensive service means we can handle Federal, State, and Administrative courts across the country.

Advanced Docket Research

With over 230 million records, Docket Alarm's cloud-native docket research platform finds what other services can't. Coverage includes Federal, State, plus PTAB, TTAB, ITC and NLRB decisions, all in one place.

Identify arguments that have been successful in the past with full text, pinpoint searching. Link to case law cited within any court document via Fastcase.

Analytics At Your Fingertips

Learn what happened the last time a particular judge, opposing counsel or company faced cases similar to yours.

Advanced out-of-the-box PTAB and TTAB analytics are always at your fingertips.

API

Docket Alarm offers a powerful API (application programming interface) to developers that want to integrate case filings into their apps.

LAW FIRMS
Build custom dashboards for your attorneys and clients with live data direct from the court.

Automate many repetitive legal tasks like conflict checks, document management, and marketing.

FINANCIAL INSTITUTIONS
Litigation and bankruptcy checks for companies and debtors.

E-DISCOVERY AND LEGAL VENDORS
Sync your system to PACER to automate legal marketing.